Timber-concrete composite beams

Mario van der Linden
Delft University of Technology / TNO Building & Construction Research

In this paper an easy-to-use design model for timber-concrete composite beams is discussed. The model is applicable for computer simulations as well as for hand calculations. A research programme was started in 1992 in co-operation with the University of Karlsruhe, to study the load-bearing capacities of timber-concrete composite beams that are subject to bending. This research programme also included shear tests, creep tests, Monte Carlo simulations on floor systems and short term tests on a platelike timber-concrete structure, that are not included in this publication.
The load-slip characteristics of three different connector types were determined and thirty bending tests, ten for each connector type, were carried out on beams constructed with these connectors.
The bending test-specimens failed due to combined bending and tensile failure of the timber, that is near knots or at a fingerjoint. Depending on the configuration of the beam and behaviour of the connectors, other phenomena could occur first. These phenomena however never initiated total collapse of the beam. Although timber beams normally exhibit brittle failure in the tensile zone, the composite beams showed a plastic behaviour before total collapse occurred. This behaviour was caused by plasticity of the connectors.
Hardly any plasticity was observed at the 5-percentile characteristic strength values for single T-beams and systems, when timber representing the Dutch strength class K17 was modelled. An elastic calculation model thus proves to be correct for most timber-concrete composite beam configurations, provided that timber beams of ordinary strength classes have been installed.
This observation is no longer valid if glulam or timber from the highest strength classes is used. It shifts the characteristic strength values upwards and plasticity of the concrete compression zone or plasticity of the connectors occurs before the timber beam with characteristic strength collapses.

Keywords: **Timber-concrete composites, connector, bending, FEM, plasticity, Monte Carlo, failure, strength, slip, stiffness**

1 Introduction

In the last decade an increasing amount of timber-concrete composite structures has been applied for the refurbishment of existing timber floors, the introduction of new floor types and as a deck system for timber bridges throughout Europe. This kind of composite structure offers benefits that depend on the kind of application. An existing timber floor can remain intact in case of refurbishment and is strengthened by adding a concrete slab. The composite system also has a positive influence on sound insulation and fire safety, apart from structural advantages. Whenever they are used for a bridge deck, they protect the timber that is positioned underneath the concrete slab from

direct sun and rain, automatically lead to diaphragm action and distribute point loads among the timber beams.

The effectiveness of a timber-concrete composite structure depends heavily on the characteristics of the shear-connector type used. No adequate design code however is available, since these characteristics and the behaviour of the composite beams constructed with them, have not been thoroughly investigated. Most research carried out so far focuses on a single project, the characteristics of a single type of connector or on theoretical design proposals that are seldom verified through full-scale tests.

The first development of a timber-concrete composite system was caused by a shortage of steel for the reinforcement of concrete after both world wars. Gerber et al (1993) mention a patent of Müller (1922) in which a system of nails and steel braces form the connection between a concrete slab and the timber.

Poštulka (1983, 1997) makes mention of more than 10,000 m^2 of timber floors that have been refurbished with the timber-concrete system in the CSSR since 1960. Nails 6.3 * 180 mm that are centred 100 mm near the supports and 250 mm at mid span, form the connection between the timber and the concrete.

Timber-concrete composite bridges that were built in New Zealand since 1970 are described by Nauta (1984). A 150 mm thick reinforced concrete slab is used where traffic is reasonably heavy. By using this type of slab in composite construction with glulam beams, the size of the beams can be reduced by 20 percent.

The first publication that combined the theory and practice of refurbishment of existing timber floors by adding a concrete slab, was by Godycki et al (1984). Thousand square metres of existing timber floor were refurbished with this method in Lodz, Poland, in 1981. Most timber beams could be reused within the composite system. The cost of the timber-concrete composite system was only half the cost of the alternative refurbishment methods.

The aim of this research was to determine an easy-to-use design model for timber-concrete composite beams, that was applicable for computer simulations as well as for hand calculations. At the start of this research programme most design proposals mentioned in literature were based on the elastic theory for composite systems, some did not even consider the slip of the joints. Additionally, the slip moduli that were sometimes derived were based on a few tests and were valid only in a small range of applications.

2 Bending tests

2.1 *Test setup and materials*

Three categories

Three timber-concrete composite beam categories were to be tested, each with a different type of connector. The concrete slab and timber beam were connected by means of:

- screws installed at ± 45°, with an interlayer of 28 mm of particleboard,
- nailplates, bent at an angle of 90°,
- reinforcement bar with a concrete notch

The three series that were tested are illustrated in figure 1.

The bending specimens were to be tested in a four-point bending test as indicated in figure 2. Each of the three categories consisted of ten bending specimens, so a total of 30 beams was tested up to failure. The estimated failure mode was rupture of the tensile zone of the timber beam, although other phenomena would then probably have occurred. These phenomena would nevertheless not immediately initiate total collapse of the beam.

An extra layer of 28 mm particleboard was placed between the timber and the concrete for the beams that were assembled with screws. This particleboard simulated flooring, which normally is present if this system is used for refurbishment purposes. The timber beam depth was set to 172 mm to maintain the same overall depth of the composite beam.

Concrete

The quality of the concrete was C25, but was not an important issue according to some initial calculations. A rise in quality of C15 up to C35 would hardly influence the behaviour of these beams. A reinforcement grid of 131 mm^2/m^1 was used to take care of the cracks that might occur due to shrinkage of the concrete in the hardening phase. This grid was positioned 30 mm above the bottom of the concrete slab.

Foil

A polyethylene (PE) foil between the timber and the concrete was used in all specimens to prevent a bond between those two materials. It also would protect the timber from the moisture that may leak from the concrete. The foil was removed at the indentations for the category bars and concrete notches. The nailplates and screws were simply driven through the foil.

Connectors

Shear tests were carried out prior to the bending tests discussed here, to obtain the load-slip characteristics of the three connector types (Blass, H.J. et al, 1995). The mean slip modulus K_s and the mean strength are presented in table 1. The results of some additional tests on screws with varying interlayer thickness are also mentioned.

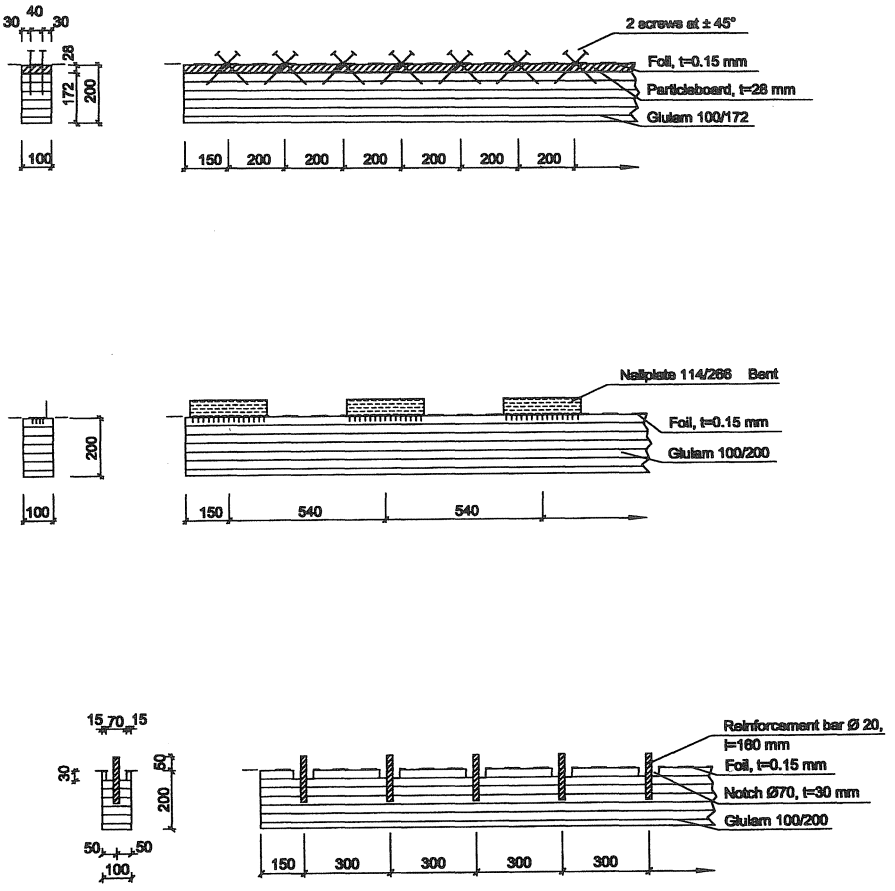

Fig.1. Dimensions of the beams and connector spacing for all bending categories.

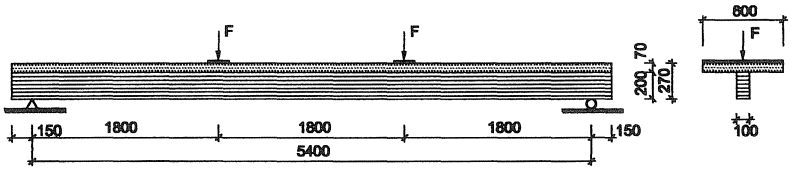

Fig. 2. Span and position of the jacks for the three categories with timber beams

Table 1. Slip modulus and strength of the connector types.

Connector type	Mean slip modulus K_s determined according to DIN EN 26891 (kN/mm)	Mean strength F_{max} (kN)	Amount of specimens tested
Screws (per pair),			
sheeting 0 mm	29.2	22.0	20
19 mm	12.9	15.3	10
28 mm	15.6	15.0	16
Nailplate	48.8	47.9	46
Reinforcement bar and concrete notch	79.5	51.1	46

The reinforcement bar and concrete notch is the strongest of the three connector types and its slip modulus is 1.6 times as large as that of the nailplates, 2.7 times as large as that of the screws without an interlayer. Nevertheless, the screws are much smaller than the other two connector types. If the strength and slip modulus of the screws is divided through its minimum spacing, thus obtaining the characteristics of a glue, the 'smeared' screws are as strong and stiff as the 'smeared' reinforcement bar and concrete notch.

The load-slip diagrams of the three connector types are shown in figure 3.

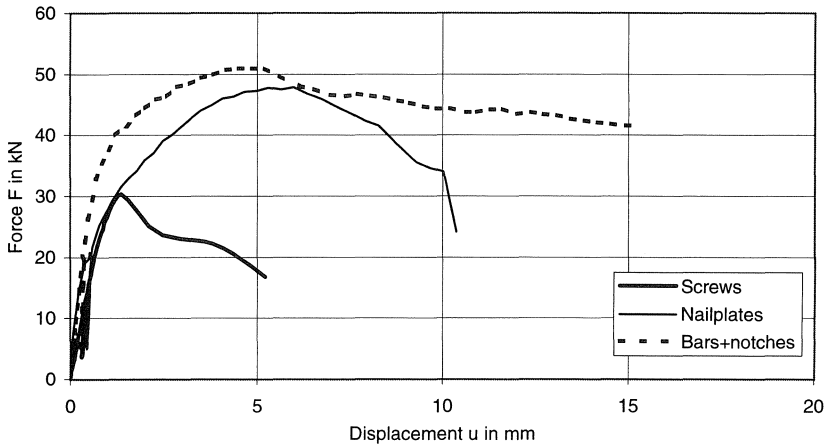

Fig. 3. Load-slip diagram of the connectors with mean load-bearing capacity for the categories screws (without sheeting), nailplates and bars and notches.

Timber

Glulam beams were used instead of sawn timber beams because they were stronger and different failure criteria were to be investigated. These criteria would sometimes arise at higher load levels which implicated higher tensile stresses in the timber beam. The moisture content appeared to be between 10 percent and 12 percent. The modulus of elasticity of the timber was set to 0.95 times the dynamic modulus of elasticity value that was obtained from measurements using natural frequency caused by longitudinal vibrations (Görlacher, 1990).

The bending strength of the timber beams could not be determined through the bending tests of the composite beam, since the exact contribution to the load-bearing capacity of the concrete slab and connectors was not specified. The only possibility to get more information on the bending strength was to make use of the modulus of elasticity and density that was measured, because they both have a relationship to the bending strength. At that time, that relationship was best described for glulam by the computer model *Karemo*, developed at the University of Karlsruhe by (Colling, 1990). The modulus of elasticity and the simulated bending strength of every timber beam are reported by (Blass, H.J. et al, 1995).

Measuring equipment

The vertical displacement at mid span, the slip along the beam axis and the deformation due to the compression stresses perpendicular to the grain at the supports, were measured besides the forces of the jacks. The slip along the beam axis was measured at the ends of the beam and at every second connector. In order to get a good estimate of the change in slip along the beam, the slip was additionally measured at each fourth or fifth connector for some specimens of each category. The same holds for the gap that might occur between the concrete and the timber at mid span. This was also measured for some specimens, but turned out to be of minor importance afterwards. The slip at the ends of the beam was determined in the beam axis, all other measurements were taken from both sides of the beam and averaged afterwards. The location of the measuring equipment is indicated in figure 4.

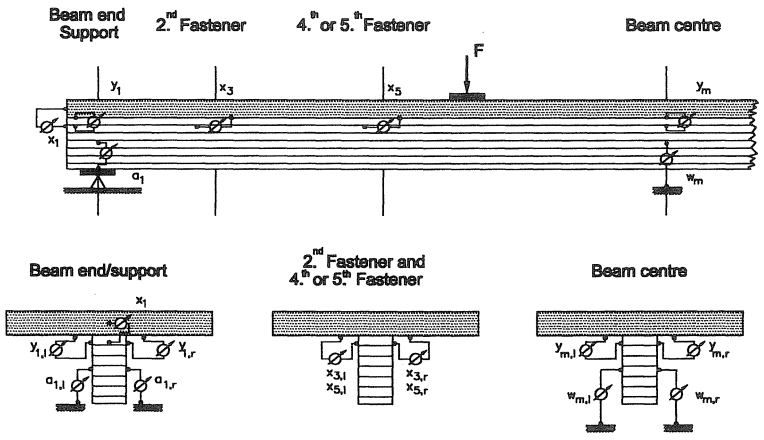

Fig. 4. Location of the measuring equipment

Test procedure

A highest load F_{est} was estimated for every category by calculation, and the specimens were initially loaded to 0.4 times F_{est}. After 30 s at this level the load was reduced to 0.1 F_{est}. Again it was held for 30 s and then increased until the test specimen failed. The displacement ratio was constantly 5.0 mm/min or 6.0 mm/min depending on the category tested, and led to a bending test that lasted between 20 and 30 minutes. The force and displacements were automatically recorded every 10 seconds. The climate of the laboratory was according to (DIN 50014 - 20/65): a temperature of 20 °C and a relative humidity of 65 percent.

2.2 *Results*

The failure modes of the test categories and the subsequent events observed during the bending tests are discussed. The load-deflection diagrams of the test specimen with about mean load-bearing capacity per category are shown in figure 5.

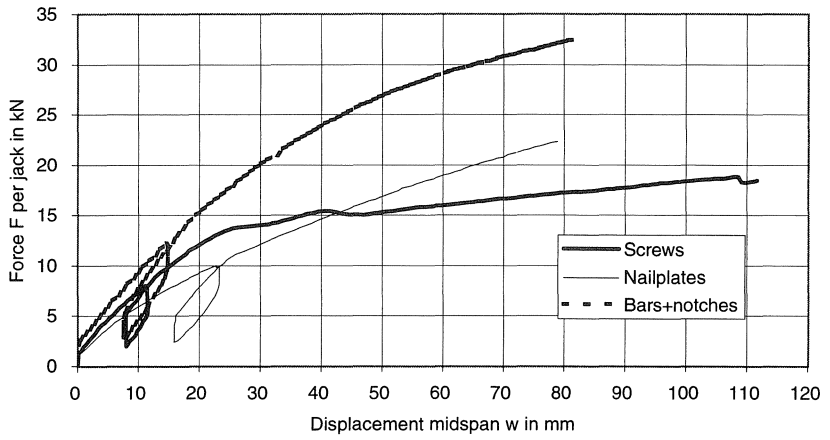

Fig. 5. Load-deflection diagram of the test specimen with mean load-bearing capacity for the categories screws, nailplates and bars and notches.

The subsequent development of local failures could roughly be observed at an increasing load:

a. Cracks occur in the tensile zone of the concrete, just underneath the jacks.
   These cracks widen and new cracks occur in the tensile zone of the concrete with increasing load.
b. A gap occurs between the timber beam and the concrete slab near one support for the category screws and bars and concrete notches, see figure 6. This gap moves towards the jacks and widens near the support with increasing loads.
d. The timber beam splits near the last connector of category bars and concrete notches. The length of the crack is about 40 mm and increases stable with increasing load. In some cases shear block failure of the concrete notch is detected, a failure mode that is similar to that of ring and shear-plate connectors in timber to timber connections.

e. A gap between the timber beam and the concrete slab sometimes occurs at the other support for the categories screws and bars and concrete notches.

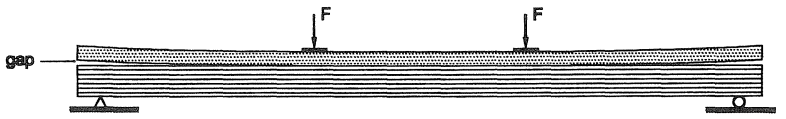

Fig. 6. Gap between the timber beam and the concrete slab at the beam ends.

f. Finally, tensile failure of the timber beam introduces total collapse of the timber-concrete composite beam.

2.3 *Conclusions*

All test-specimens finally failed due to failure of the timber, that is near knots or at a fingerjoint. Depending on the configuration of the beam and behaviour of the connectors, other phenomena could occur first, like plasticity of the connectors, cracks in the concrete tensile zone and so on. These phenomena in contrast never initiated total collapse of the beam. The timber beams failed in bending. One of the strongest timber beams failed due to the shear stresses at middepth, that reached the shear strength.

Although timber beams normally exhibit brittle failure in the tensile zone, the composite beams showed a plastic behaviour before total collapse occurred. This behaviour was caused by the connectors that had an elasto-plastic load-slip relationship. Once the outer connectors reached their maximum shear strength, redistribution took place to the adjacent connectors until they also became plastic. In this way the interlayer between the concrete and the timber lost its initial stiffness and sometimes became fully plastic.

The three categories cannot be compared to each other directly, since they differed in the number of connectors utilised and in the depth of the timber beam. The only statement that can be made is that all categories satisfied the requirements for serviceability and ultimate limit state. Table 2 gives an overview of the maximum loads that were measured, the standard deviation is also mentioned. This last parameter is merely an indication with only ten specimens per category. The maximum load is the load per jack, the total load on the beam should therefore be multiplied by two.

Table 2. Maximum load per jack for each category.

Category	Mean (kN)	Standard deviation (kN)	Amount of specimens
Screws	19.1	2.2	10
Nailplates	23.3	4.5	9
Bars and notches	32.3	3.5	10

For the category nailplates the first beam failed due to a badly glued fingerjoint in the outer lamella. This beam is not taken into account in this category.

The connectors were placed such that the end distance equalled 150 mm for the category with reinforcement bars and concrete notches, see figure 1. The end distance for ring connectors is twice the diameter according to (Eurocode 5, 1994) and 2.3 times the diameter according to (NEN 6760, 1990) that results in 140 and 160 mm respectively. Obviously this value is critical due to the cracks and shear block failure that was observed near the beam ends. Although this kind of failure is not critical for the total beam failure, the end distance should be taken larger to prevent splitting of the timber.

3 Calculation models

3.1 General

The bending tests described in paragraph 2 clearly show that a linear model is not able to determine the load-carrying capacity accurately for the configurations tested, as non-linearities almost certainly influence the behaviour at higher load levels.

Simple linear models that take into account the slip between the elements of a composite beam, are described by many authors. For instance, by Werner (1992) and are based on prior work of Möhler (1956) and Newmark et al (1951). Stüssi (1947) was the first to come up with a linear model that is widely used nowadays. Amana et al (1967) and Goodman et al (1968) derived a model for three layers. Schelling (1968) extended the former theories to beams with more than three layers and interlayer slip. So far, all of the models assume linear material behaviour, a negligible shear deformation and a simply supported beam. Heimeshoff (1991) described an approximation for a beam with three supports and different load conditions, Aicher et al (1987) also took into account the shear deformations for sandwich structures subjected to bending moments.

Although an elastic model is not supposed to give good approximations of the failure load after plasticity has occurred, a model comparable with Möhler's model (1956) was derived to determine the amount of deviation between model and bending tests. This model is described in paragraph 3.2. Additionally, an extension was made to the model, which led to the 'frozen shear force' model described in paragraph 3.3.

A model based on the Finite Element Method (FEM) was also developed to simulate the bending tests and to account for the nonlinear material behaviour. This model, that is discussed in paragraph 3.4, is the most extensive one.

3.2 *Elastic analytical model*

The model discussed in this paragraph is closely related to Möhler's model (1956). The basic assumptions of this model are:

1. A linear elastic material behaviour is assumed for the concrete and the timber, cracking and plasticity are thus not taken into account.
2. The connectors are equally spaced.
3. All connectors have the same load-slip relationship that is schematized as linear elastic up to the load-bearing capacity of the connector and from that point on ideal plastic, see figure 7b. In this model only the elastic part is used and a maximum strength is not given, see figure 7a. Each connector type is only described by its slip modulus K.

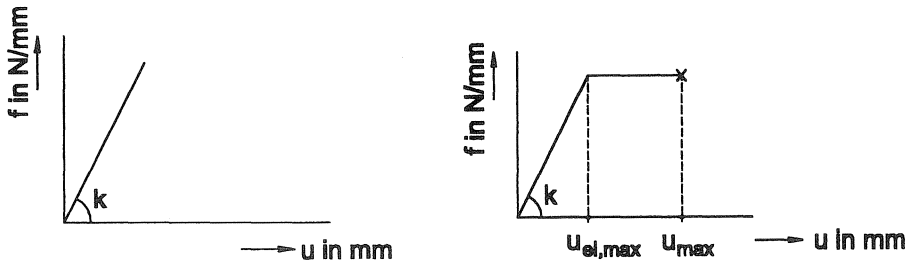

a. b.

Fig. 7. Behaviour of the connectors: a. elastic, b. elasto-plastic.

4. The discrete connectors are assumed to act as a continuous connection, called "smeared" connectors, with slip modulus *k*.
5. The friction between the timber and the concrete is not considered. The shear force in the interlayer is totally taken by the connectors.

Equilibrium between the internal and external forces of figure 8 yields

$$\sum F_z(x) = 0 \Rightarrow \frac{dQ_c(x)}{dx} + \frac{dQ_t(x)}{dx} = -q(x) \tag{1}$$

$$\sum F_x(x) = 0 \Rightarrow \frac{dN_c(x)}{dx} + \frac{dN_t(x)}{dx} = 0 \tag{2}$$

$$\sum M_A(x) = 0 \Rightarrow \frac{dM_c(x)}{dx} + \frac{dM_t(x)}{dx} - \frac{1}{2}h\frac{dN_c(x)}{dx} = Q_c(x) + Q_t(x) \tag{3}$$

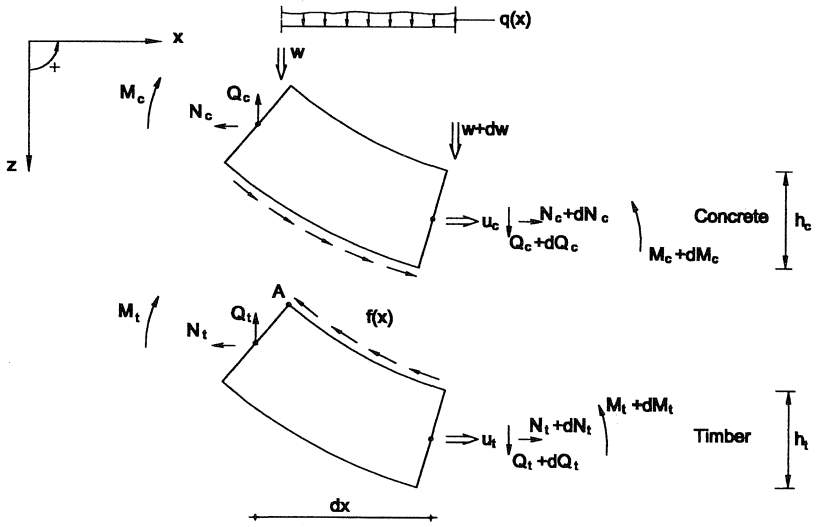

Fig. 8. Part of the composite beam loaded by q(x).

These three equilibrium equations were combined with the constitutive equations for normal force and bending of the two elements, resulting in

$$(EI_c + EI_t)\frac{d^4w(x)}{dx^4} + \frac{1}{2}EA_c \cdot h\frac{d^3u_c(x)}{dx^3} = q(x) \tag{4}$$

The contribution of the normal forces in each component is given by

$$-EA_c\frac{d^2u_c(x)}{dx^2} = k\ \ u(x) = k(u_t(x) - u_c(x)) + \frac{1}{2}kh\frac{dw(x)}{dx} \tag{5}$$

$$-EA_t\frac{d^2u_t(x)}{dx^2} = k\ \ u(x) = k(u_t(x) - u_c(x)) + \frac{1}{2}kh\frac{dw(x)}{dx} \tag{6}$$

which results in three equations with three parameters to be solved:
. w(x), the deflection in z-direction
. u_c(x), the displacement at the centre of gravity of the concrete in x-direction, and
. u_t(x), the displacement at the centre of gravity of the timber in x-direction.

A simple closed form solution is obtained for a load

$$q(x) = q_0 \sin\left(\frac{\pi}{l} \cdot x\right) \tag{7}$$

By stating

$$w(x) = C_1 \sin\left(\frac{\pi}{l} \cdot x\right) \tag{8}$$

the constant C_1 is calculated as

$$C_1 = \frac{q_0 l^4}{\pi^4 E I_{ef}} \tag{9}$$

with

$$EI_{ef} = E_{t,d}[I_{tot} + \gamma \cdot (nA_c e_c^2 + A_t e_t^2)] \tag{10}$$

The second moment of plane area I_{tot} is written as

$$I_{tot} = I_t + nI_c \tag{11}$$

and

$$\gamma = \frac{1}{1+p} \tag{12}$$

where

$$p = E_{c,d}\left(\frac{\pi}{l}\right)^2 \frac{1}{k} \frac{A_t A_c}{A_t + nA_c} \tag{13}$$

$$n = \frac{E_{c,d}}{E_{t,d}} \tag{14}$$

and the eccentricities of the concrete slab e_c and timber beam e_t are represented by

$$e_c = \tfrac{1}{2} h \frac{A_t}{A_t + nA_c} \tag{15}$$

$$e_t = \tfrac{1}{2} h \frac{nA_c}{A_t + nA_c} \tag{16}$$

Where h is the total depth of the composite beam, A_c, A_t, e_c and e_t are indicated in figure 9.

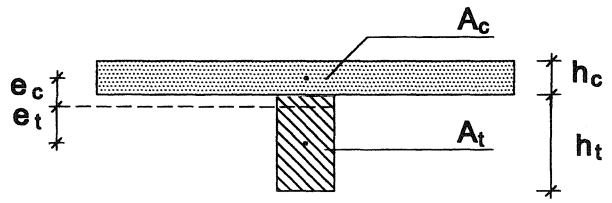

Fig. 9. Eccentricities and cross sectional areas of the concrete slab and timber beam.

The smeared slip modulus k equals:

$$k = \frac{K}{s} \tag{17}$$

in which the mean spacing of the connectors s is given by:

$$s = 0.75\ s_{min} + 0.25\ s_{max} \tag{18}$$

if s varies uniformly in the longitudinal direction according to the shear force, and s_{max} is lessthan four times s_{min}, according to Eurocode 5 (1994). The connectors should be regarded to be positioned in one row, with a fictitious spacing s, if more than one row of connectors is present.

The bending strength $f_{t,m}$ in the outermost fibre of the timber tensile zone, is reached at a sine load level

$$q_{f_{t,m}} = \frac{\frac{\pi^2}{l^2}}{\frac{\left(1 - \frac{EI_{min}}{EI_{ef}}\right)}{\frac{1}{2}hA_t} + \frac{E_t h_t}{2EI_{ef}}} \cdot f_{t,m} \tag{19}$$

3.3 *Frozen shear force model*

A new calculation method was introduced to calculate the failure load of a timber-concrete composite beam, once the first connectors have reached plasticity. This method considers the plasticity of the connectors by the assumption of an elasto-plastic load-slip diagram, as presented in figure 7b. The approach leads to lower bound solutions assuming that a linear material behaviour of the concrete and timber is still a valid starting-point. If tests show that the non-linear material behaviour of these materials strongly influences the load levels discussed here, the derived equations no longer represent lower bound solutions. The real material behaviour would then induce lower load-bearing strengths.

The basic idea behind this approach is to freeze the shear forces in all connectors when the first one at the support starts to yield. The interlayer is now assumed to be fully plastic, although this plasticity is set to a different load level for each individual connector. The level of plasticity coincides with the shear force that is present in each connector at the time the first connector reaches its real level of plasticity. A sine-function of the load introduces a cosine distribution of these shear forces as indicated in figure 10. The model is discussed in more detail in (Van der Linden, 1999)

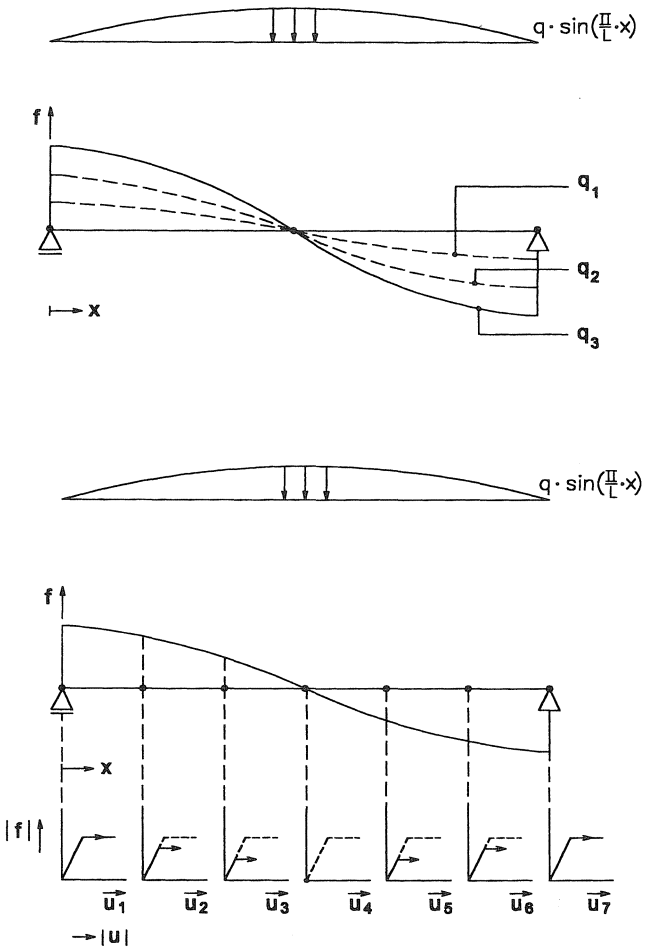

Fig. 10. Distribution of the shear forces in the interlayer with increasing load according to a linear behaviour of the connectors (above) and at 'frozen' levels (below).

3.4 FEM *model*

Three parts of the simulation model

The simulation model developed during this research, consists of three parts. In the first part, the input phase, all relevant material data, the configuration of the beam and the desired accompanying output can be specified. The model is able to take care of the statistical distributions of the timber, considering the correlation between the material parameters. This is done by means of a multivariate random distribution programme (RANLIB). The model then automatically generates the mesh and appropriate input for the DIANA program, a finite element method (DIANA, 1992). However, a deterministic simulation of a single test also can be carried out, by overruling the random routines for the Monte Carlo calculation by the input of a single beam.

In the second part of the model a bending test can be simulated and the load-displacement diagram up to failure is obtained by successive non-linear load steps. This simulation can be performed for a single beam, but also for a total floor system.

The third part of the model is a post-processor of the DIANA program that stores the relevant output of the single calculation. The next simulation is started if a distribution of the load-carrying capacity of the floor system is desired.

Configuration and elements used

The Finite Element part of the model (DIANA, 1992) consists of three kinds of elements that are used to describe the timber-concrete composite T-beam. Shell elements were used to model the concrete slab, spring elements for the connectors between the concrete and the timber, and beam elements were used for the timber, see figure 11.

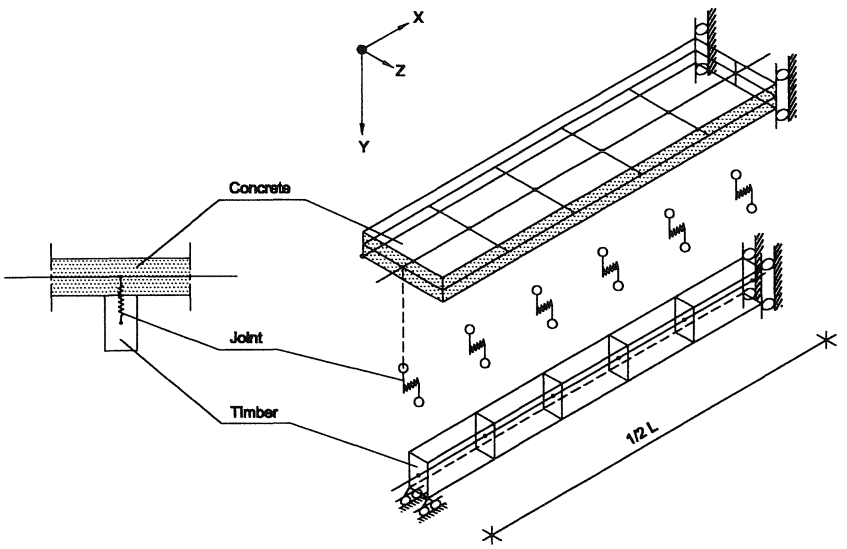

Fig. 11. Finite Element model of a timber-concrete composite beam.

Reinforcement was not modelled in the FEM model. The reinforcement is often placed at the centre of the concrete and hardly raises the load-bearing capacity of the concrete. The main reason for using reinforcement is often to prevent cracks due to shrinkage of the concrete. The net steel section is thus minimum, resulting in minor forces contributing to the strength of the timber-concrete composite beam.

Crack criterion for the timber

A brittle crack criterion was used in the tensile zone of the timber. When a crack occurred in one of the integration points of an element, the remaining integration points of that element were given a tensile strength of five percent of the original value. A crack thus would propagate upwards, resulting in the 'loss' of that element and consequently of the total beam if only a single beam was considered. This extension was modelled to simulate unstable crack growth that was often observed in bending tests on timber beams.

4 Simulations

4.1 *General*

A Monte Carlo simulation was carried out with the FEM model, simulating a hundred bending tests on each category, to obtain the distribution of the failure loads (Van der Linden, 1996). The simulation nearest to the mean value of each distribution is the simulation that is focused upon.
The figures that are demonstrated in the following paragraphs, display the load-deflection diagram of the test-specimen nearest to the mean load-bearing capacity obtained in the tests, and that of each calculation model, representing about the mean load-bearing capacity of its category. The bending stiffness of the test-specimen consequently deviates from the mean value since a single test-specimen cannot embody every mean material characteristic. A direct comparison between the 'mean' test specimen and each 'mean' calculation is therefore not entirely possible.

Simplicity was the main goal for all calculation models that were derived. Even for the FEM model the input was kept to a minimum for instance, by just characterising the load-slip diagram of the connectors by two or three straight lines. A better approximation would without doubt have been obtained with a more complex FEM model, but this was not the intention of this research. One should keep these assumptions in mind when the models are compared to the test results.

4.2 *Simulation of the bending tests*

Beams with screws

The linear part of the load-deflection diagram of the models is in close agreement with that of the test-specimen, see figure 12. The analytical 'frozen shear force' model starts to deviate from the elastic stiffness at the same load as found in the bending tests. The FEM model slightly overestimates this bending point. The analytical model then starts to overestimate the real behaviour, mainly because the model assumes 'frozen' plasticity of the connectors where a decreasing load-slip diagram is present in reality. Apart from that, the concrete tensile zone remains linear elastic and is not able to crack in this model. The interlayer of 28 mm of particleboard is modelled via an extra depth of 28 mm that was added to the timber beam, because the model could only represent two layers of material. These factors also contribute to the overestimation of the load-bearing capacity and bending stiffness.

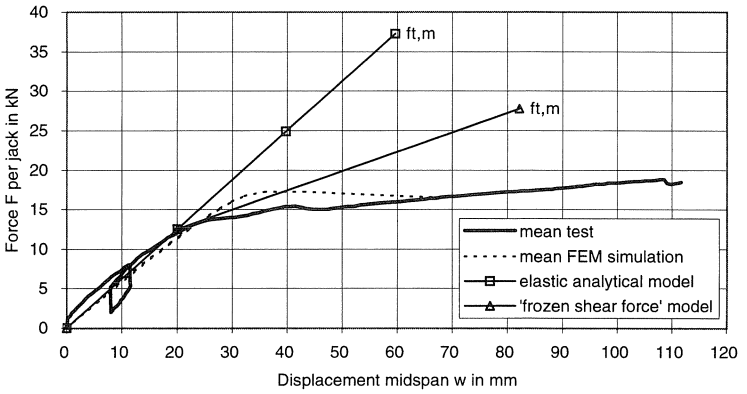

Fig. 12. Load-deflection diagrams representing the mean load-bearing capacity of the category screws.

The FEM model considers cracking and the decreasing shear force that is transferred by the connectors at higher slip values, and consequently determines a smaller bending stiffness than the analytical model does. The first cracks in the concrete arise at 14.3 kN; in the tests they were noticed at 13–15 kN.

The mean load-bearing capacity as calculated by the FEM model, underestimated the mean load-bearing capacity by eleven percent. This might be the result of the way in which the connectors are modelled at slip-deformations larger than 6 mm. Slip values of about 15 mm were recorded at failure, the connector force at this level was not known since the shear tests were stopped at a slip of about 6 mm. Additional FEM simulations with an ideal plastic behaviour of the screws, showed that the load-bearing capacity could be raised by a maximum of 40 percent. The additional simulations show the importance of the load-slip characteristics of the connectors, even after they have reached their maximum load-bearing capacity.

Beams with nailplates

The load-deflection diagram of the test-specimen bends off earlier than both calculation models do, see figure 13. This deviation is caused by the way in which the connectors are modelled. The load-slip characteristics of the nailplate are simulated by just one or two straight lines up to the maximum load-bearing capacity of the connector. This simplified nailplate behaviour results in a different reduction of the bending stiffness between the mean FEM simulation and the mean test.

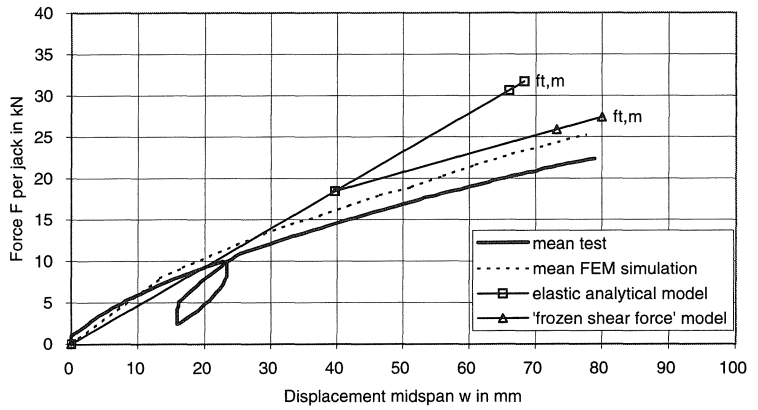

Fig. 13. Load-deflection diagrams representing the mean load-bearing capacity of the category nailplates.

The behaviour is captured almost correct once the bending stiffness remains constant: the load-deflection paths are parallel up to failure of the timber beam. The first concrete crack occurs in the FEM model at 12.7 kN, whereas it was observed at 8-15 kN in the tests. The displacement reached at failure is predicted very well by both models, but the load-bearing capacity is overestimated by fifteen percent, also due to the deviation in behaviour that is calculated in the first part of the diagram.

Beams with reinforcement bars and concrete notches

The load-deflection diagrams presented in figure 14 almost lead to the same observations that were made for the nailplates. The load-deflection diagram of the test-specimen bears off earlier than both calculation models do. Again, substituting the real load-slip behaviour of the connectors by just one or two straight lines results in the deviation that is found. The first concrete crack occurs in the FEM model at 23.4 kN, whereas it was 12-22 kN in the test-specimens.

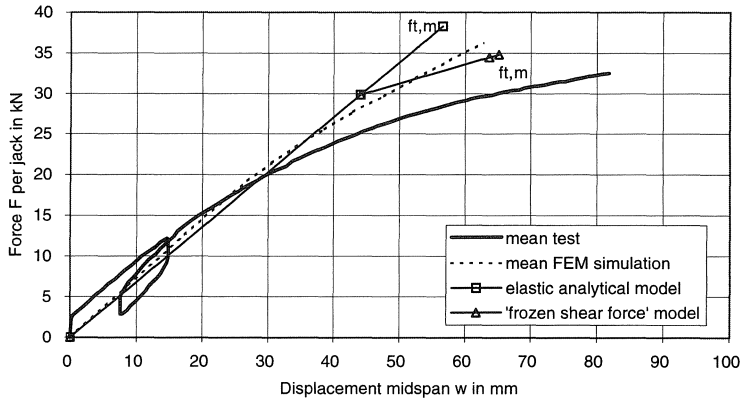

Fig. 14. Load-deflection diagrams representing the mean load-bearing capacity of the category reinforcement bars and concrete notches.

The behaviour is captured satisfactorily once the bending stiffness remains almost constant: the load-deflection paths are parallel up to failure of the timber beam. The displacement reached at failure is underestimated by both models, the load-bearing capacity is overestimated by twelve percent.

4.3 *Conclusions and discussion*

The first deviation from linear elastic behaviour that occurs in the bending tests and in the FEM model, is cracking of the concrete near the loading points. The model then predicts plasticity in the compression zone of the concrete which is hard to observe at the test beams. This could however be correct because the calculated concrete strain is about 2 - 2.5‰ at failure load, which probably is too small to observe plasticity at the beams. Between or after that, depending on the characteristics of the connector, the connectors start to yield. In both test and FEM simulation the ultimate load-bearing capacity is reached when the bending strength of the timber is reached. Plasticity in the compression zone of the timber is not observed in the bending tests. According to the calculation models plasticity might occur for the T-beams at higher load levels, but should normally not be expected.

The calculation models seem to show a stiffer behaviour of the timber-concrete composite beams than determined at the test-specimens at higher load levels. This difference might occur due to creep deformations that arose in the tests and that are not incorporated in the calculation models. Since the bending tests lasted between 20 and 30 minutes, creep deformations might have occurred.

Additional simulations carried out with a ten percent lower bending strength, could explain another phenomenon that occurred in the Monte Carlo simulations as well. In most categories it was observed that the distribution of the ultimate loads per category could differ from a normal distribution, although the input parameters had been assigned normal distributions. This skewness is likely to be caused by the plasticity of the connectors in the timber-concrete composite beams. Plasticity of the connectors is not reached for timber beams having a low bending strength, and the stresses in the materials are still linear elastic at failure of the timber beam. The connectors become plastic if the timber beam is much stronger and thus the load on the timber-concrete composite beam can be increased. It then depends on the configuration how much the ultimate load can be increased. The ultimate load nearly remained constant for the screws category and was raised for the other categories. It is this behaviour for beams having higher bending strengths, that results in the skewness of the distributions at higher load levels.

The mean test results are best described by the FEM model, although the "frozen shear force" model also gives a good estimate of the mean failure loads. The load-deflection diagrams simulated by the FEM model give the best approximation of the real behaviour, but this model also is the most laborious one for the user. The deviations from the real failure loads are mainly caused by the quality of the input parameters for the timber beam, that were obtained through indirect methods. The mean failure loads as determined through the calculation models, are expressed as a ratio to the mean failure load obtained from the tests and presented in table 3.

The "frozen shear force" model shows the largest discrepancy for the category screws. The model assumes full plasticity of the connectors. If a declining load-slip behaviour is present, as is true for the category screws, the model overestimates the load-bearing capacity. In those circumstances the plasticity level of the connector has to be chosen such that it represents the mean shear force transferred in that range of slips. This modification was not carried out for the calculations described in this paragraph, but it would have led to a ratio closer to one in table 3.

Table 3. Ratio of the mean calculated failure load to the mean failure load obtained through the bending tests.

Category: Calculation model:	Screws	Nailplates	Reinforcement bars and concrete notches
FEM model	0.89	1.15	1.12
elastic analytical model	1.96	1.36	1.19
"frozen shear force" model	1.45	1.18	1.08

5 Structural behaviour at a lower timber quality

A design model for timber-concrete composite beams should be able to describe the plastic structural behaviour that was observed in the bending tests. This can be concluded from the former paragraph, in which the FEM model and the 'frozen shear force' model more accurately described the failure loads than the elastic analytical model.
However, the bending tests were performed on composite beams that were assembled with glulam beams. Glulam is stronger and its modulus of elasticity is higher than that of ordinary sawn timber. It is thus somewhat premature to recommend a plastic design model based on tests that incorporated timber of higher qualities. Sawn timber is what is usually present in projects that need to be refurbished.

Additional simulations were carried out on timber-concrete composite beams that were assembled with sawn timber of an ordinary Dutch strength class, K17. A Monte Carlo simulation was carried out for a hundred beams per configuration, storing the behaviour up to failure of each beam. The distribution of the failure loads was thus obtained and the 5-percentile characteristic strength values were determined.

One of these simulated configurations, series 3 that is comparable to the composite beams with nailplates described in 2.1, is discussed in more detail.
The intention of these simulations was to model configurations at the limit of what could possibly be achieved with sawn timber. So the results obtained from the nailplate configuration should not directly be compared to the results of series 3. The load-deflection diagram of three characteristic strength levels is presented in figure 15.

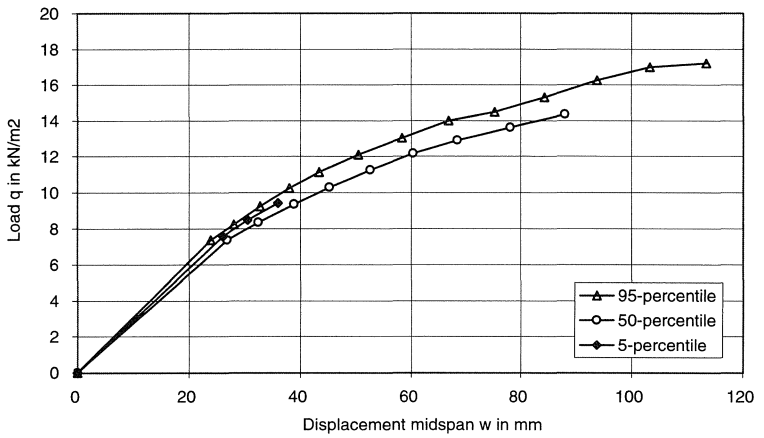

Fig. 15. Load-displacement diagrams for series 3.

The 50- and 95-percentile simulations still show a plastic behaviour, comparable to the results of the bending tests. The bending strengths of the timber beams were 29 and 43 N/mm^2 respectively. These values are of the same magnitude as the strengths of the glulam beams used in the bending tests; consequently the same kind of plastic behaviour arises for these percentiles.

The 5-percentile simulation, at a timber bending strength of only 21 N/mm^2, showed a linear behaviour. Apparently the timber beam failed before the connectors were able to become plastic. This behaviour at the 5-percentile characteristic strength level was observed for all configurations simulated, provided that a certain amount of composite behaviour was present. Composite beams without or with only minor interaction, could show a plastic behaviour of the connectors, even at this load level. However, these beams were merely simulated to study the influence of the connectors and did not represent a system to be used in common practice.

6 Conclusions

The bending test-specimens failed due to rupture of the tensile zone of the timber beam, that is near knots or at a fingerjoint. Depending on the configuration of the beam and behaviour of the connectors, other phenomena could occur first, like plasticity of the connectors, cracks in the concrete tensile zone and so on. These phenomena in contrast never initiated total collapse of the beam.

Although timber beams normally exhibit brittle failure in the tensile zone, the composite beams showed a plastic behaviour before total collapse occurred. This behaviour was caused by the connectors that had an elasto-plastic load-slip relationship. Once the outer connectors reached their maximum shear strength, redistribution took place to the adjacent connectors until they also became plastic.

The Monte Carlo calculations that simulated the manufacturing and testing of composite beams and floor systems, revealed a skewness in the distribution of the failure loads of each category. The highest failure loads sometimes hardly differed from the mean failure loads, due to plasticity of the connectors that occurred at higher load levels. Consequently, the assumption of a normal distribution for the strength of a timber-concrete composite configuration often turns out to be wrong.

The test results are best described by the FEM model, although the 'frozen shear force' model also gives a good estimate of the failure loads. The load-deflection diagrams simulated by the FEM model give the best approximation of the real behaviour, but this model also is the most laborious one for the user. The deviations from the real failure loads are mainly caused by the quality of the input parameters for the timber beam, that were obtained through indirect methods.

A linear calculation model is recommended for the design of timber-concrete composite beams, if the timber beam belongs to a regular strength class for sawn timber (Blass, H.J. et al, 1996). The simulations show that no or hardly any plasticity occurs at the 5-percentile characteristic load-bearing capacity. At this load level the timber beam fails before any plasticity is able to occur.

If the connectors turn out to have become plastic and the concrete and timber still behave linear elastic, then the 'frozen shear force' model described in paragraph 3.3 can be used. The connectors become plastic before the timber beam fails, for instance, in composite beams with minor interaction.

More advanced design tools, like the FEM model discussed in paragraph 3.4, should only be used if the nonlinear behaviour of the timber beam or concrete slab influences the load-bearing capacity. This is the case when glulam beams or sawn timber of the highest strength classes are used.

Notations

Symbol	Description	Dimension
Latin		
A	Cross sectional area	mm^2
EA_c	Resistance to elongation of the concrete slab	N
EA_t	Resistance to elongation of the timber beam	N
EI_{ef}	Effective bending stiffness of the composite beam	N/mm^2
EI_c	Bending stiffness of the concrete slab	Nmm^2
EI_t	Bending stiffness of the timber beam	Nmm^2
EI_{min}	Minimum bending stiffness of the composite beam	Nmm^2
F	Load	kN
F_{est}	Estimated highest load	kN
I	Second moment of plane area	mm^4
K	Slip modulus	N/mm

K_s	slip modulus according to DIN EN 26891	N/mm
M	Bending moment	kNm
N	Normal force	kN
Q	Shear force	kN
e	eccentricity	mm
f	smeared connector forces between the timber and the concrete	N/mm
$f_{t,m}$	timber bending strength	N/mm^2
h	depth of the timber-concrete beam	mm
h_c	depth of the concrete slab	mm
h_t	depth of the timber beam	mm
k	smeared slip modulus, defined as K/s	N/mm/mm
l	span	mm
n	ratio modulus of elasticity of concrete to modulus of elasticity of timber	–
q	distributed load	kN/m, kN/m^2
s	spacing of the connectors	mm
s_{max}	maximum spacing of the connectors	mm
s_{min}	minimum spacing of the connectors	mm
u	displacement in x-direction	mm
u_c	displacement at the centre of gravity of the concrete	mm
$u_{el,max}$	maximum elastical slip of a connector	mm
u_{max}	maximum slip of a connector at failure	mm
u_t	displacement at the centre of gravity of the timber	mm
w	displacement in z-direction	mm

Greek

γ	combination factor that shows the effectiveness of the connections in a composite beam ($0 < \gamma < 1$)

Subscripts

c	concrete, compression
d	design value
ef	effective
el	elastic
m	bending
max	maximum
min	minimum
mod	modification
t	timber
x	parallel to the x axis
z	parallel to the z axis

References

AICHER, S. and VON ROTH, W., Ein modifiziertes γ-Verfahren für das Mechanische Analogon: dreischichtiger Sandwichverbund - zweiteiliger verschieblicher Verbund. Bautechnik 1. 1987

AMANA, E.J. and BOOTH, L.G., Theoretical and experimental studies on nailed and glued plywood stressed-skin components: Part 1, Theoretical Study, Journal of the Institute of Wood Science Vol. 4, No. 1, 1967

AMANA, E.J. and BOOTH, L.G., Theoretical and Experimental studies on nailed and lued plywood stressed-skin components: Part 2, Experimental Study, Journal of the Institute of Wood Science Vol. 4, No. 2, 1967

BLASS, H.J.; EHLBECK, J.; VAN DER LINDEN, M.L.R.; SCHLAGER, M. Trag- und Verformungsverhalten von Holz-Beton-Verbundkonstruktionen, Universität Fridericiana Karlsruhe, Versuchsanstalt für Stahl, Holz und Steine, 1995

BLASS, H.J.; SCHLAGER, M; VAN DER LINDEN, M.L.R.; Trag- und Verformungsverhalten von Holz-Beton-Verbundkonstruktionen, Bauen mit Holz, Teil 1, 5/96 und Teil 2, 6/96

COLLING, F., Tragfähigkeit von Biegeträgern aus Brettschichtholz in Abhängigkeit von den festigkeitsrelevanten Einflußgrößen, Dissertation, Universität Karlsruhe, 1990.

DIN 50014. Klimate und ihre technische Anwendung; Normalklimate. Juli 1985.

DIN EN 26891 Holzbauwerke; Verbindungen mit mechanischen Verbindungsmitteln, Allgemeine Grundsätze für die Ermittlung der Tragfähigkeit und des Verformungsverhaltens. Juli 1991

Eurocode 5. Design of timber structures. Part 1-1: General rules and rules for buildings. NVN-ENV 1995-1-1, first print, June 1994

GERBER, C., QUAST, U., STEFFENS, R., Balkenschuhe als Verbundmittel für Holzbalkendecken mit mittragender Stahlbetondecke. Beton- und Stahlbetonbau 88, Heft 9, 1993

GODYCKI, T.; PAWLICA, J.; KLESZCZEWSKI, J. Verbunddecke aus Holzrippen und Betonplatte. Bauingenieur 59, 1984

GOODMAN, J.R. and POPOV, E.P., Layered beam systems with interlayer slip. Journal of the

Structural Division, ASCE Vol. 94, No. ST11, Proc. Paper 6214, pp 2535-2547, 1968

GÖRLACHER, R., Klassifizierung von Brettschichtholzlamellen durch Messung von Longitudinalschwingungen. Dissertation, Universität Karlsruhe, 1990.

HEIMESHOFF, B., Näherungsverfahren zur Berechnung von Einfeldträgern mit Kragarm und von Zweifeldträgern, die aus nachgiebig miteinander verbundenen Querschnittsteilen bestehen, im Ingenieurholzbau, Holz als Roh- und Werkstoff 49, pp 277-285, 1991

MÖHLER, K., Über das Tragverhalten von Biegeträgern und Druckstäben mit zusammengesetztem Querschnitt und nachgiebigen Verbindungsmitteln. Habilitation TH Karlsruhe, 1956

MÜLLER, P., Decke aus hochkantig stehenden Holzbohlen oder Holzbrettern und Betondeckschicht. Patentschau aus dem Betonbau und den damit verwandten Gebieten. Auszüge aus den Patentschriften. Beton und Eisen, H. XVII, S. 244, 1922

NATTERER, J. and HOEFT, M., Zum Tragverhalten von Holz-Beton Verbundkonstruktionen. Forschungsbericht CERS Nr. 1345. EPFL/IBOIS March 1987

NAUTA, F., New Zealand Forest Service Timber Bridges. Proceedings of 1984 Pacific Timber Engineering Conference, Auckland, New Zealand, 1984

NEN 6702;1991 Belastingen en vervormingen, TGB 1990
TGB 1990 Loadings and deformations
NEN 6760;1991 Houtconstructies, TGB 1990
TGB 1990 Timber structures
NEWMARK, N.M., SIESS, C.P., and VIEST, I.M., Tests and analysis of composite beams with incomplete interaction. Proceedings, Society for Experimental Stress Analysis, Vl. 9, No. 1, pp 75-92, 1951
POŠTULKA, J. Strengthening of Wooden Ceiling Constructions. IABSE Symposium Strengthening of Building Structures - Diagnosis and Therapy, Venezia, 1983
POŠTULKA, J. Holz-Beton-Verbunddecken, 36 Jahre Erfahrung. Bautechnik 74, 1997
SCHELLING, W., Die Berechnung nachgiebig verbundener, zusammengesetzter Biegeträger im Ingenieurholzbau. Dissertation TH Karlsruhe, 1968
STÜSSI, F., Zusammengesetzte vollwandträger. International Association for Bridge and Structural Engineering, IABSE, Vol. 8, pp 249-269, 1947
VAN DER LINDEN, M.L.R., Monte Carlo simulations of timber-concrete composite beam tests. Report no. 25.4.96.3/HC-12, Delft University of Technology, March 1996
VAN DER LINDEN, M.L.R., Timber-concrete composite floor systems. Delft University of Technology, Ph.D.Thesis, 1999
WERNER, H., Holz-Beton-Verbunddecke mit einer neuartigen Fugenausbildung. Bauen mit Holz Nr. 4, 1992

Computer programs used:

DIANA, User's Manual - Release 5.1, Revision A - April 29, 1992
Volume 0 - Introduction & Utilities
Volume 1 - Linear Static Analysis
Volume 4 - Nonlinear Analysis

The Multi-Variate Programme used is public domain software and retrieved from:

RANLIB
Library of Fortran Routines for Random Number Generation
compiled and written by: Barry W.Brown / James Lovato
Department of Biomathematics, The University of Texas, M.D. Anderson Cancer Center. This work was supported by grant CA-16672 from the National Cancer Institute.

Reference for some subroutines involved:

Subroutines Spofa and Sdot used by setgmn:
Dongarra, J.J., Moler, C.B., Bunch, J.R. and Stewart, G.W.,
Linpack User's Guide. STAM Press, Philadelphia, 1979
Bottom level routines:
L'Ecuyer, P. and Cote, S., Implementing a Random Number Package with Splitting Facilities, ACM Transactions on Mathematical Software, 17:98-111, 1991